Translational Science

Cancer Research

CD44-Targeting PLGA Nanoparticles Incorporating Paclitaxel and FAK siRNA Overcome Chemoresistance in Epithelial Ovarian Cancer

Yeongseon Byeon[1], Jeong-Won Lee[2], Whan Soo Choi[1], Ji Eun Won[1], Ga Hee Kim[1], Min Gi Kim[1], Tae In Wi[1], Jae Myeong Lee[1], Tae Heung Kang[1], In Duk Jung[1], Young-Jae Cho[2], Hyung Jun Ahn[3], Byung Cheol Shin[4], Young Joo Lee[5], Anil K. Sood[6,7,8], Hee Dong Han[1], and Yeong-Min Park[1]

Abstract

Chemotherapy is commonly used in the treatment of ovarian cancer, yet most ovarian cancers harbor inherent resistance or develop acquired resistance. Therefore, novel therapeutic approaches to overcome chemoresistance are required. In this study, we developed a hyaluronic acid-labeled poly(d,l-lactide-co-glycolide) nanoparticle (HA-PLGA-NP) encapsulating both paclitaxel (PTX) and focal adhesion kinase (FAK) siRNA as a selective delivery system against chemoresistant ovarian cancer. The mean size and zeta potential of the HA-PLGA-NP were 220 nm and -7.3 mV, respectively. Incorporation efficiencies for PTX and FAK siRNA in the HA-PLGA-NPs were 77% and 85%, respectively. HA-PLGA-NP showed higher binding efficiency for CD44-positive tumor cells as compared with CD44-negative cells. HA-PLGA (PTX+FAK siRNA)-NP caused increased cytotoxicity and apoptosis in drug-resistant tumor cells. Treatment of human epithelial ovarian cancer tumor models HeyA8-MDR ($P < 0.001$) and SKOV3-TR ($P < 0.001$) with HA-PLGA (PTX+FAK siRNA)-NP resulted in significant inhibition of tumor growth. Moreover, in a drug-resistant, patient-derived xenograft (PDX) model, HA-PLGA (PTX+FAK siRNA)-NP significantly inhibited tumor growth compared with PTX alone ($P < 0.002$). Taken together, HA-PLGA-NP acts as an effective and selective delivery system for both the chemotherapeutic and the siRNA in order to overcome chemoresistance in ovarian carcinoma.

Significance: These findings demonstrate the efficacy of a novel, selective, two-in-one delivery system to overcome chemoresistance in epithelial ovarian cancer. *Cancer Res; 78(21); 6247–56. ©2018 AACR.*

Introduction

Ovarian cancer is the leading cause of death from gynecological malignancies in women because of its high recurrence rate and eventual resistance to cytotoxic chemotherapy (1, 2). Chemotherapeutic drugs are commonly used for the treatment of ovarian cancer; however, most cancers have developed inherent or acquired resistance, highlighting the need for novel therapeutic approaches to overcome chemoresistance and to improve treatment outcomes.

Several nanoparticle (NP) platforms have been extensively developed to overcome drug resistance (3–6). NP-based drug delivery systems are highly attractive in cancer therapy due to their specific capacities and biocompatibilities (3, 7, 8). In addition, NPs increase the concentration of therapeutic payloads at disease sites, thereby minimizing concerns regarding unexpected side effects.

Poly(d,l-lactide-co-glycolide) (PLGA) polymer is particularly attractive for clinical and biological applications, given its low toxicity, low immunogenicity, biocompatibility, and biodegradability. PLGA has been used extensively in NP carrier systems encapsulating payloads (9, 10). In addition, hyaluronic acid (HA) has been shown to function as a ligand against the CD44 receptor, which is expressed on the surfaces of tumor cells. Moreover, HA provides conformational stability and improves binding selectivity for CD 44 receptors (11, 12).

[1]Department of Immunology, School of Medicine, Konkuk University, Chungju, South Korea. [2]Department of Obstetrics and Gynecology, Samsung Medical Center, Sungkyunkwan University School of Medicine, Seoul, South Korea. [3]Center for Theragnosis, Biomedical Research Institute, Korea Institute of Science and Technology, Seoul, South Korea. [4]Bio/Drug Discovery Division, Korea Research Institute of Chemical Technology, Daejeon, South Korea. [5]Department of Bioscience and Biotechnology, Sejong University, Seoul, South Korea. [6]Department of Gynecologic Oncology and Reproductive Medicine, The University of Texas MD Anderson Cancer Center, Houston, Texas. [7]Center for RNAi and Non-coding RNA, The University of Texas MD Anderson Cancer Center, Houston, Texas. [8]Department of Cancer Biology, The University of Texas MD Anderson Cancer Center, Houston, Texas.

Note: Supplementary data for this article are available at Cancer Research Online (http://cancerres.aacrjournals.org/).

Y. Byeon, J.-W. Lee, and W.S. Choi contributed equally to this article.

H.D. Han and Y.-M. Park share senior authorship of this article.

Corresponding Authors: Hee Dong Han, Konkuk University, 268 Chungwondae-Ro, Chungju, Chungcheong-Buk-Do 380-701, South Korea. Phone: 82-2-2030-7848; Fax: 82-2-2049-6192; E-mail: hanhd@kku.ac.kr; and Yeong-Min Park, Phone: 82-2-2049-6158; Fax: 82-2-2049-6192; E-mail: immun3023@kku.ac.kr

doi: 10.1158/0008-5472.CAN-17-3871

Among many novel targets for chemoresistance, focal adhesion kinase (FAK) is considered attractive for therapeutic development. Increased FAK expression has been reported in a number of tumor types, including breast (13), colon (14), and ovarian (15) cancers. In addition, FAK inhibition sensitizes cancer cells to chemotherapy (16, 17). FAK plays an important role in many malignant features, including tumor invasion, migration, and survival, and elevates the expression of drug efflux pumps (18), leading to FAK induced chemoresistance. In recent years, siRNA-based approaches using NP delivery systems have been used extensively in cancer therapy to silence the expression of specific genes such as FAK (7, 19, 20).

Here, we developed HA-labeled PLGA NPs (HA-PLGA-NPs) incorporating both paclitaxel (PTX) and FAK siRNA as a two-in-one delivery system to increase the efficiency of targeted delivery against tumor-specific receptors and to enhance therapeutic efficacy in chemoresistant ovarian cancer. In the present study, we demonstrated the highly selective delivery of targeted NPs into CD44 receptor-positive cells and the therapeutic efficacy of this approach in chemoresistant epithelial ovarian cancer (EOC) models and in a human ovarian patient-derived xenograft (PDX) model (21, 22). This approach provides a new combination for chemotherapy and gene silencing to overcome chemoresistance in EOC.

Materials and Methods

Materials

Paclitaxel (PTX, Mw 853.906 Da) was purchased from Samyang Biopharmaceuticals Co. Poly(d,l-lactide-co-glycolide) acid (PLGA, Resomer RG502H, monomer ratio 50:50, Mw 10–12 kDa) was purchased from Boehringer Ingelheim (Ingelheim, Germany). Poly(vinyl alcohol) (PVA, 80% hydrolyzed, Mw 9–10 kDa) and FAK inhibitor (1,2,4,5-benzenetetraamine tetrahydrochloride, Mw 284.01 Da) were purchased from Sigma-Aldrich Co. Hyaluronic acid (HA, Mw 5–150 kDa) was purchased from Tokyo Chemical Ind. Ki67 and CD31 antibodies were purchased from Abcam. FAK, AKT, and p-AKT antibodies were purchased from Cell Signaling Technology. Terminal deoxynucleotidyl transferase dUTP nick end labeling (TUNEL) assay kit was purchased from Trevigen (TACS 2 TdT DAB Kit). All other materials were of analytical grade and were used without further purification.

Preparation of HA-PLGA-NPs

We prepared HA-PLGA-NPs incorporating both PTX and siRNA by a water-in-oil-in-water (w/o/w) double emulsion solvent evaporation method (10). Briefly, 125 μg of siRNA was dissolved in 0.2 mL deionized water as a first water phase and treated with 2 mL chloroform containing 900 μg PTX and 40 mg PLGA using a probe-type sonicator (Sonics, USA) at 4°C for 1 minutes (20 pulses of 5 s with 3 s gaps). The primary emulsion was further emulsified with a secondary water phase (500 μg HA dissolved in 10 mL of 2.0% w/v PVA) at 4°C for 10 min. Chloroform in the emulsion was evaporated using a rotary evaporator at 30°C under vacuum. After evaporation, unbound PVA or HA was removed by centrifugation at 13,000 rpm for 20 minutes and further washed 3 times to isolate HA-PLGA-NPs. The resultant HA-PLGA-NPs were stored at 4°C until use.

The size and surface charge of PLGA-NP were measured by dynamic light scattering using an electrophoretic light scattering photometer (SZ-100, Horiba; refs. 10, 23). The morphology of HA-PLGA-NP was observed with scanning electron microscopy (SEM, Tescan Mira 3 LMU FEG, Brno, Czech Republic).

The encapsulation of PTX into the HA-PLGA-NPs was confirmed by H-NMR (500 MHz, HRMAS-FT-NMR, Bruker, Germany; Supplementary Fig. S1) and the encapsulation efficiency assessed by high performance liquid chromatography (HPLC; 1200 Series HPLC System, Agilent; ref. 24). The encapsulation efficiency of FITC-labeled siRNA into HA-PLGA-NPs was determined by a UV-visible spectrophotometer at 488 nm (7). To determine the labeling efficiency of HA onto the HA-PLGA-NPs, we conjugated FITC onto HA using a chemical modification (Supplementary Fig. S2A and S2B). The labeling efficiency of FITC-labeled HA onto HA-PLGA-NPs was determined by a UV-visible spectrophotometry at 488 nm.

Cell lines and siRNA

The derivation and source of human epithelial ovarian cancer cell lines A2780, A2780-CP20 (cisplatin resistant), SKOV3, SKOV3-TR (PTX resistant), HeyA8, and HeyA8-MDR (multidrug resistance) have been previously described (A.K. Sood, MD Anderson Cancer Center, 2014; refs. 16, 19). Cells were maintained in RPMI 1640 medium supplemented with 0.1% gentamycin (Sigma-Aldrich) and 10% FBS (Biowest, Nuaille, France). The cells were routinely tested for the absence of *Mycoplasma* and virus infections for hepatitis and sendai from Korea Research Institute of Bioscience and Biotechnology (Ref. No. M16543, South Korea). The cells were free of *Mycoplasma* and inspected at 2016. All *in vitro* and *in vivo* experiments were conducted when cells reached 70% and 80% confluency at passage 5. Control siRNA (sense: TTCTCCGAACGTGTCACGT, anti-sense: ACGTGACACGTTCGGAGAA), FAK siRNA (sense: GUAUUGGACCUGCGAGGGA, anti-sense: UCCCUCGCAGGUCCAAUAC), and survivin siRNA (sense: CAGACUUGGCCCAGUGUUU, anti-sense: AAACACUGGGCCAAGUCUG) were purchased from Sigma-Aldrich.

Intracellular uptake of HA-PLGA-NPs

We confirmed the *in vitro* selective intracellular delivery of HA-PLGA-NPs that occurs through the targeting of CD44 receptors on the cell surface using confocal microscopy (LSM710, Carl Zeiss; ref. 25). Before confirming selective delivery, we first selected CD44-positive cells by flow cytometry (BD FACSCalibur flow cytometer, BD Biosciences) using FITC-CD44 antibody (eBioscience). The fluorescent dye, tetramethylrhodamine (TRITC, Sigma-Aldrich) was used as a model drug and was encapsulated into PLGA-NPs and HA-PLGA-NPs in a second emulsion procedure. The encapsulation efficiency of TRITC was determined via UV-visible spectrophotometry at 562 nm (Supplementary Fig. S3). Tumor cells were then incubated with TRITC-encapsulated HA-PLGA-NPs for 30 minutes at 37°C, washed in cold PBS, fixed with 4% (w/v) paraformaldehyde solution for 15 minutes at 25°C, and stained with 1 μmol/L Sytox green (Life technologies) in PBS for 10 minutes. Intracellular delivery of the TRITC-encapsulated HA-PLGA-NPs was determined using fluorescence images obtained via confocal microscopy.

Cell viability assay

Following treatment of the tumor cells with HA-PLGA (PTX)-NPs with or without FAK siRNA, cell viability was determined

using an MTT assay (26). Untreated cells were seeded in 96-well plates in triplicates, incubated for 24 hours at 37°C and 5% CO_2. After incubation, cells were washed and treated with FAK siRNA to silence the FAK. The cells were then allowed to incubate for 48 hours, after which, they were washed and incubated for 72 hours with medium containing HA-PLGA (PTX)-NPs with or without FAK siRNA. Cell viability was determined via MTT assay.

Apoptosis assay

The relative percentage of apoptotic cells was assessed using an Annexin V-FITC apoptosis detection kit (BD Biosciences; ref. 22). Briefly, tumor cells were treated with FAK siRNA for 48 hours and replated onto 6-well plates. HA-PLGA (PTX)-NPs were then added to the medium and the cells were further incubated for 72 hours. After incubation, the cells were treated with Annexin-V-PE and/or 7-ADD for 15 minutes. The number of apoptotic cells was evaluated using a BD FACSCalibur flow cytometer and CELLQuest software (22).

In vivo selective delivery of HA-PLGA (PTX+siRNA)-NPs in a mouse model

Receptor-targeted delivery of the NPs was assessed as previously described (7). CD44-positive, HeyA8-bearing mice were given a single injection of either nontargeted PLGA (PTX+siRNA)-NPs or targeted HA-PLGA (PTX+siRNA)-NPs, both labeled with FITC. The mice were then sacrificed and tumor tissues were harvested. The efficiency of the targeted delivery was determined from the percentage of FITC-labeled NPs located in the tumor tissue, when observed in five random fields.

Orthotopic *in vivo* model of ovarian cancer and tissue processing

Female BALB/c nude mice (6–7 weeks old, 25 g) were purchased from Orient (Gapyeong, South Korea). All procedures and maintenance conditions were approved by the Konkuk University Institutional Animal Care and Use Committee (Ref. No.: KU17188). Mice were housed in a specific pathogen-free housing facility at Konkuk University. To produce tumors, HeyA8-MDR or SKOV3-TR cells (1×10^6 cells per 0.2 mL HBSS) were injected into the peritoneal cavity of the mice ($n = 10$ mice per group). The mice were monitored daily for adverse effects and sacrificed when control group mice seemed moribund.

NP treatment began 1 week after the injection of tumor cells into the mice. Each control group [PLGA (control siRNA)-NPs], PTX alone, PLGA (PTX)-NPs, PLGA (siRNA)-NPs, PLGA (PTX+siRNA)-NPs, and HA-PLGA (PTX+siRNA)-NPs was given twice weekly via intravenous injection at a dose of 200 μg/kg (siRNA) and 1.4 mg/kg (PTX) based on body weight. Treatment continued until the control group mice became moribund (typically 4 to 5 weeks), at which point all the mice were sacrificed. Mouse weight, tumor weight, number of nodules, and tumor distribution were recorded immediately. The clinicians who performed necropsies, tumor collections, and tissue processing were blinded to the treatment group assignments. Tissue specimens were fixed either with formalin or optimum cutting temperature (OCT, Miles, Inc.) or were snap frozen.

Real time quantitative RT-PCR

Relative expression of FAK and survivin mRNA in mice after treatment was determined by real-time quantitative RT-qPCR with 50 ng of RNA that was isolated from treated tumor tissue using an RNeasy Mini Kit (Qiagen). Relative expression values were obtained using the $2^{-\Delta\Delta CT}$ method and normalized to the control value to obtain percent fold changes (7, 19).

IHC staining

IHC analyses were conducted on tumor tissues treated with HA-PLGA (PTX+siRNA)-NPs. Analysis of cell proliferation (Ki67), microvessel density (MVD and CD31), and FAK expression (FAK antibody) were performed as previously described (7, 16). All analyses were recorded in 5 random fields for each slide. In addition, TUNEL assay was performed to determine cell apoptosis (19). Apoptotic cells were quantified by counting the number of apoptotic cells in 5 random fields. All staining analyses were quantified by 2 blinded investigators.

Therapeutic efficacy of HA-PLGA (PTX+siRNA)-NPs in an ovarian cancer PDX model

To establish a PDX model of ovarian cancer, surgical tumor specimens of the patient were sliced into small pieces (less than 2–3 mm), implanted into the subrenal capsule of mice left kidneys, and propagated by serial transplantation (21, 22). The mice were then randomly allocated to the following treatment groups ($n = 10$ mice per group): (i) 1.4 mg/kg PTX, (ii) PLGA (PTX+FAK siRNA)-NPs, and (iii) HA-PLGA (PTX+FAK siRNA)-NPs (1.4 mg/kg PTX+200 μg/kg FAK siRNA). Mice in both NP treatment were groups received treatment twice weekly via intravenous injection. Treatment continued until the control group mice became moribund (27).

Statistical analysis

Differences between groups in terms of continuous variables were analyzed using the Student *t* test. ANOVA was performed to compare differences between multiple groups. A value of $P < 0.05$ was considered statistically significant.

Results

Characteristics of HA-PLGA (PTX+siRNA)-NPs

We chose CD44 as a target receptor given its selective overexpression in ovarian cancer cells. We used HA as a targeting ligand that can bind specifically to the CD44 receptor (11). In addition, we chose PLGA, which is particularly attractive for clinical and biological applications, as the polymer matrix (10). We then prepared HA-PLGA-NPs using a w/o/w double emulsion method to encapsulate both PTX and FAK siRNA. We first determined the physical properties of PLGA-NPs, PLGA (PTX)-NPs, PLGA (siRNA)-NPs, PLGA (PTX+siRNA)-NPs, and HA-PLGA (PTX+siRNA)-NPs (Fig. 1). The mean particle size and zeta potential were approximately 220 ± 5.69 nm and −7.3 ± 0.73 mV, respectively (Fig. 1A and B). The encapsulation of PTX in HA-PLGA (PTX+siRNA)-NPs was confirmed by H-NMR (Supplementary Fig. S1). As shown in Supplementary Fig. S1, the peaks for the CH of the benzene group (i) in PTX and CH_3 of the methylene group (ii) in PLGA were observed at 7–8 ppm and 1–2 ppm, respectively. In addition, HA labeling on the surface of HA-PLGA (PTX+siRNA)-NPs was determined by measuring UV absorbance using FITC-conjugated HA (Supplementary Fig. S2A and S2B). We next measured PTX encapsulation into HA-PLGA (PTX+siRNA)-NPs by HPLC. The loading efficiencies of PTX and siRNA were 77.7% and 85.0%, respectively (Fig. 1C and D). Representative histograms of the NP size distributions

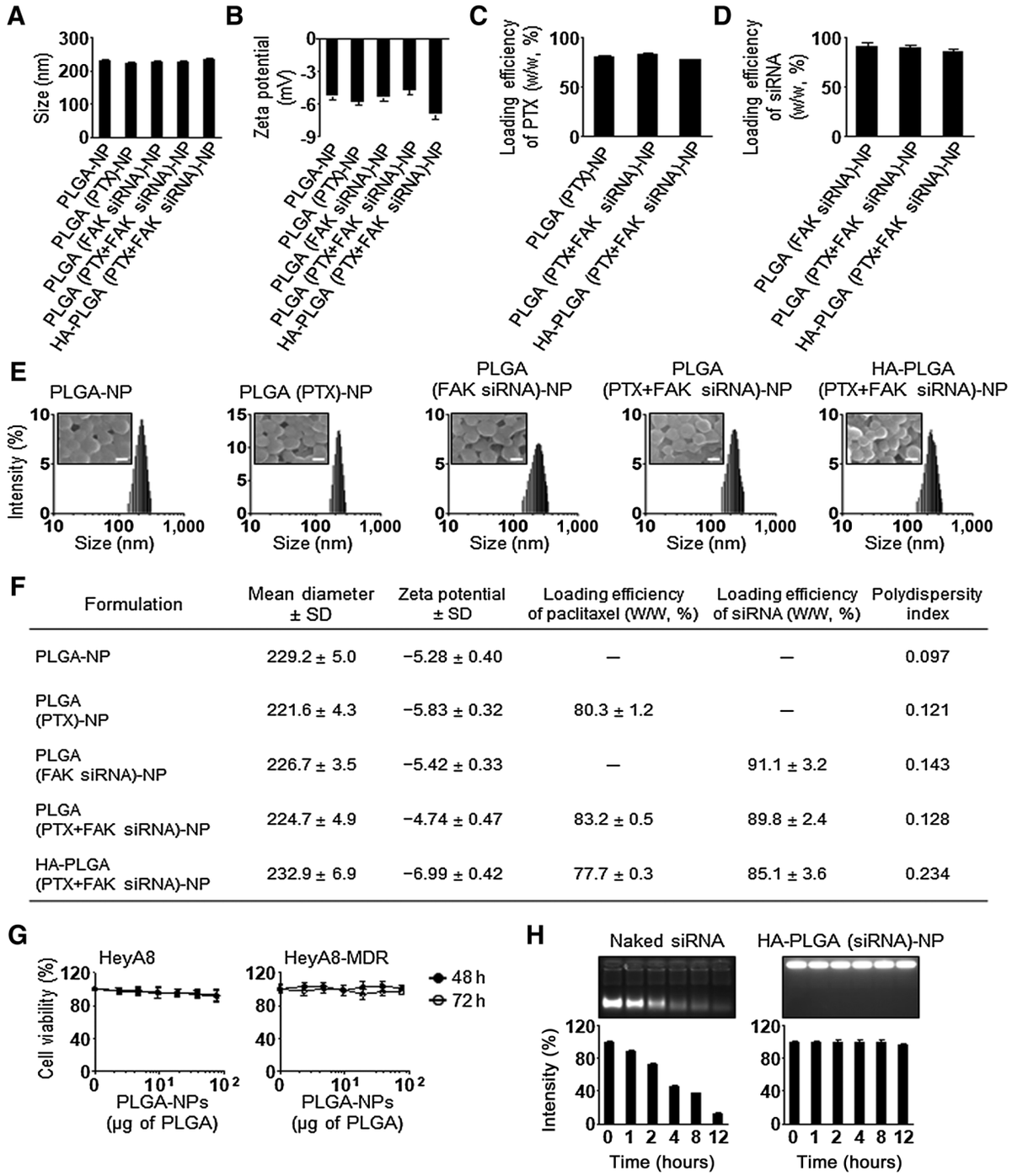

Figure 1.

Physical properties of HA-PLGA-NPs. **A** and **B,** Size (**A**) and surface charge (**B**). **C** and **D,** Loading efficiency of PTX (**C**) and FAK siRNA (**D**) into PLGA-NPs. Loading efficiency of PTX into PLGA-NPs was determined by HPLC, whereas that of siRNA was determined by measuring the fluorescence intensity of FITC-labeled siRNA at 488 nm. **E,** Size distribution and morphology of PLGA-NPs. Morphologies of PLGA-NPs were observed by SEM. **F,** Physical properties of PLGA-NPs. **G,** Cell viability of HA-PLGA-NPs without PTX and siRNA in tumor cells was assessed via MTT assay. **H,** Electrophoretic migration of HA-PLGA (siRNA)-NPs in 50% serum. HA-PLGA (siRNA)-NPs were collected at different times after incubation at 37°C. Scale bar, 200 nm; error bars, SEM.

(200–220 nm) are shown in Fig. 1E, and their spherical morphologies were confirmed by SEM. Consequently, physicochemical properties of PLGA-NPs are shown in Fig. 1F. Moreover, we assessed the cytotoxic effect of PLGA-NPs without encapsulation of PTX and siRNA against tumor cells (Fig. 1G). Cell viability was 95% even with increasing PLGA concentration, indicating that the

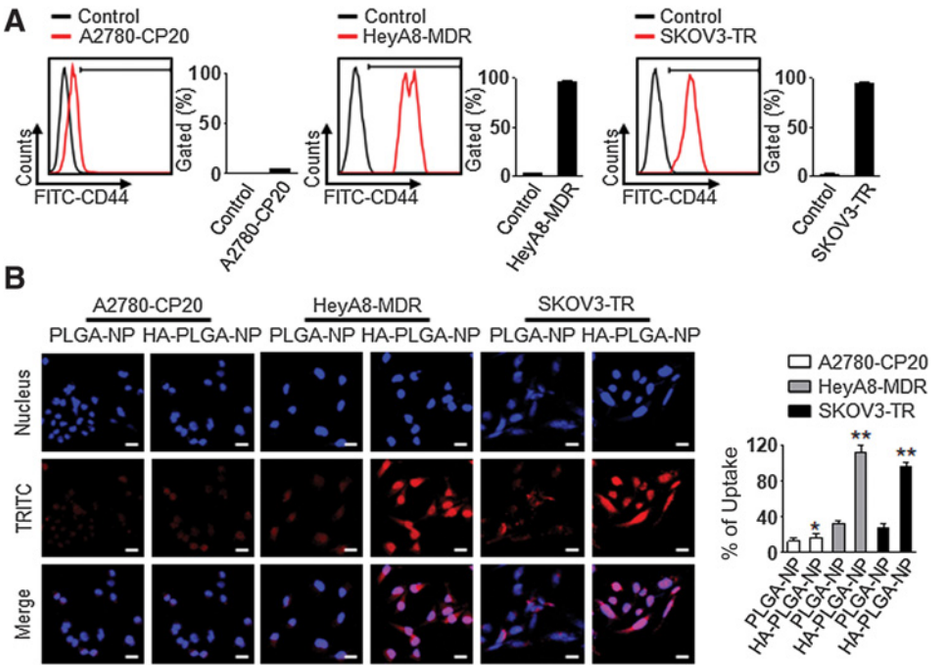

Figure 2.
Selective intracellular delivery of PLGA-NPs or HA-PLGA-NPs against ovarian tumor cells. **A,** CD44 expression of A2780-CP20, HeyA8-MDR, and SKOV3-TR cells by flow cytometry using FITC-labeled CD44 antibody. **B,** CD44-mediated intracellular delivery of HA-PLGA-NPs in ovarian tumor cells. Cells were fixed in 4% paraformaldehyde and their nuclei (blue) stained with Sytox green for 10 minutes. The intracellular delivery was analyzed by confocal microscopy (scale bar, 20 μm). Quantitative differences were analyzed by fluorescence intensity of TRITC (red)/Sytox green (blue). Error bars, SEM. *, $P < 0.07$; **, $P < 0.01$.

PLGA-NPs failed to induce any cytotoxic effect in the tumor cells. We next confirmed the stability of PLGA (siRNA)-NPs under serum conditions. Although naked siRNA was degraded, siRNA incorporated into HA-PLGA (siRNA)-NPs did not degrade when placed in serum for more than 12 hours (Fig. 1H).

Selective delivery of HA-PLGA-NPs to CD44 receptor–expressing tumor cells

Before evaluating the efficacy of delivery, we assessed CD44 expression in ovarian cancer cell lines by flow cytometry. Although A2780 and A2780-CP20 cells were did not express CD44, HeyA8, HeyA8-MDR, SKOV3, and SKOV3-TR cells showed expressed CD44 on the cell surface (Fig. 2A; Supplementary Fig. S4). On the basis of these result, we selected specific CD44-positive and CD44-negative cell lines for subsequent experiments. In addition, we evaluated CD44 expression in normal and tumor patient tissues via IHC staining and fluorescence microscopy (Supplementary Fig. S5).

We next confirmed the selective delivery efficiency of TRITC encapsulated HA-PLGA-NPs into drug-resistant ovarian tumor cells (A2780-CP20, HeyA8-MDR, and SKOV3-TR) via fluorescence microscopy (Fig. 2B). As expected, lower binding was observed in A2780-CP20 cells because of its CD44-negative expression. However, HA-PLGA-NPs increased binding efficiency in CD44-positive Hey8-MDR and SKOV3-TR cells. In addition, we confirmed the binding of HA-PLGA-NPs to drug-sensitive ovarian tumor cell lines (A2780, HeyA8, and SKOV3). HA-PLGA-NPs showed higher binding efficiency in CD44-positive HeyA8 and SKOV3 cells compared with that in CD44-negative A2780 cells (Supplementary Fig. S6).

Assessment of cell viability and apoptosis

After treatment with HA-PLGA (PTX)-NPs with or without FAK siRNA, we assessed *in vitro* cell viability for drug-resistant HeyA8-MDR and SKOV3-TR cells. Treatment with the combination of HA-PLGA (PTX)-NPs and FAK siRNA induced significant cell death compared with HA-PLGA (PTX)-NPs without FAK siRNA (Fig. 3A and B). We next assessed apoptosis of cells mediated by HA-PLGA (PTX)-NPs with FAK siRNA. In comparison with treatment with HA-PLGA (PTX)-NPs without FAK siRNA, administration of the combination of HA-PLGA (PTX)-NPs and FAK siRNA induced a significant increase in the apoptosis of HeyA8-MDR and SKOV3-TR cells (Fig. 3C and D). AKT activation contributes to metastasis and resistance to chemotherapy (28). Therefore, we evaluated AKT activation after FAK silencing (Supplementary Fig. S7) and saw that FAK silencing decreased pAKT expression. Therefore, FAK silencing in taxane-resistant tumor may contribute to drug sensitization by decreasing pAKT expression. In addition, we confirmed the cell viability and apoptosis of drug-sensitive HeyA8 and SKOV3 cell lines (Supplementary Fig. S8). Treatment with HA-PLGA (PTX)-NPs with FAK siRNA showed similar cell viability and apoptosis compared with HA-PLGA (PTX)-NPs without FAK siRNA, because of drug sensitive cell lines.

In vivo targeted delivery of HA-PLGA-NPs to tumor tissues

Before performing proof-of-concept for *in vivo* efficacy studies, we tested the extent of *in vivo* delivery following a single intravenous injection of FITC-labeled HA-PLGA-NPs into HeyA8-bearing mice. After harvesting, we stained the tumors for CD44 to evaluate colocalization of HA-PLGA-NPs. HA-PLGA-NPs (green) were consistently colocalized (yellow) with CD44 receptors (red) in tumor tissues (Fig. 4). These findings indicate that HA-PLGA-NPs were selectively delivered into CD44-positive cells.

Therapeutic efficacy of HA-PLGA (PTX + siRNA)-NPs in an orthotopic EOC model

To determine the potential therapeutic efficacy against drug-resistant tumors, we focused on the protein FAK, because it plays a significant role in drug resistance (29). Thus, we used the drug

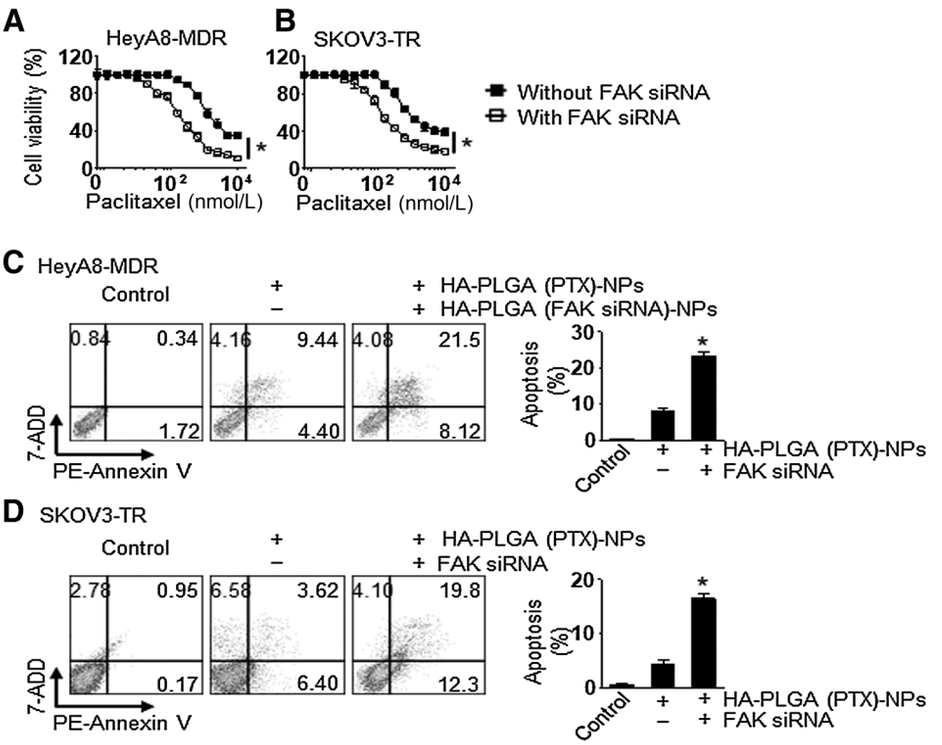

Figure 3.
Cell viability and apoptosis assays of drug-resistant tumor cells after treatment with HA-PLGA-NPs. Cell viability after treatment with HA-PLGA-NPs with or without FAK silencing was determined by MTT assay. **A** and **B,** HeyA8-MDR (**A**) and SKOV3-TR (**B**). **C** and **D,** Apoptosis assay of HeyA8-MDR (**C**) and SKOV3-TR (**D**) cells treated with HA-PLGA-NPs with or without FAK silencing for 72 hours. Bar graph represents the mean of three independent tests. Error bars, SD. *, $P < 0.05$. Statistical tests were two-sided and P values were evaluated using Student t test.

resistant, FAK-positive, HeyA8-MDR and SKOV3-TR tumor models for our study (Supplementary Fig. S9). Seven days following the injection of tumor cells into the peritoneal cavity, mice were randomly allocated to the following groups ($n = 10$ mice/group): (i) control [PLGA (control siRNA)-NPs], (ii) PTX alone, (iii) PLGA (PTX)-NPs, (iv) PLGA (FAK siRNA)-NPs, (v) PLGA (PTX+FAK siRNA)-NPs, and 6) HA-PLGA (PTX+FAK siRNA)-NPs. FAK siRNA (200 μg/kg) and/or PTX (1.4 mg/kg) were injected intravenously into the mice twice a week. In the HeyA8-MDR model, treatment with HA-PLGA (PTX+FAK siRNA)-NPs resulted in a significant inhibition of tumor growth compared with treatment with PLGA (PTX+FAK siRNA)-NPs (64% reduction, $P < 0.04$) or the control (88% reduction, $P < 0.001$, Fig. 5A). HA-PLGA (PTX+FAK siRNA)-NPs also induced a significant decrease in the number of nodules compared with the control (80% reduction, $P < 0.01$, Fig. 5A). After treatment, the decrease in FAK mRNA levels was confirmed by qRT-PCR (Fig. 5A). HA-PLGA (PTX+FAK siRNA)-NPs induced a significant reduction in the expression of FAK mRNA compared with PLGA (PTX+FAK siRNA)-NPs (48% reduction, $P < 0.03$) and to the control (83% reduction, $P < 0.001$). Additionally, mice treated with HA-PLGA (PTX+FAK siRNA)-NPs had a 60% chance of survival for at least 50 days compared with the control and other treatment groups where all the mice died within 45 days (Fig. 5A). Moreover, we confirmed the presence of multiple tumor nodules in the tumor-bearing mice after they were sacrificed (Fig. 5B). We further confirmed the off target effect of control siRNA and FAK siRNA with different sequences (Supplementary Fig. S10A and S10B).

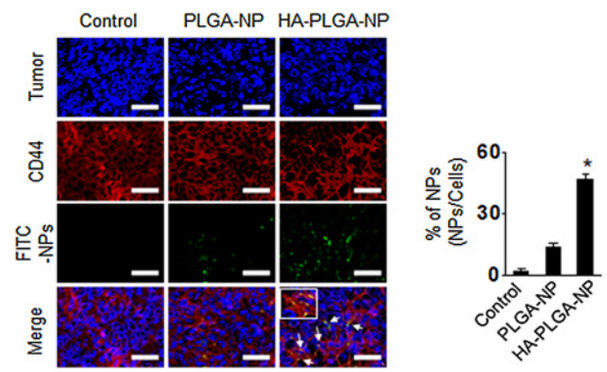

Figure 4.
In vivo delivery of FITC-labeled HA-PLGA-NPs. Tumor tissues were harvested after single injection of either PLGA-NPs or HA-PLGA-NPs into HeyA8-bearing mice. Colocalization of FITC-labeled HA-PLGA-NPs (green) and CD44 receptor (red) in tumor tissues were detected by fluorescence microscopy (scale bar, 25 μm). Error bars, SEM. *, $P < 0.05$.

In the SKOV3-TR model, HA-PLGA (PTX+FAK siRNA)-NPs treatment induced a significant inhibition in tumor growth compared with PLGA (PTX+FAK siRNA)-NPs treatment (49% reduction, $P < 0.01$) or control (73% reduction, $P < 0.001$, Fig. 5C). HA-PLGA (PTX+FAK siRNA)-NP treatment also resulted in a significant inhibition in the number of nodules compared with the control (73% reduction, $P < 0.01$, Fig. 5C). After treatment, the decrease in FAK mRNA levels was confirmed by qRT-PCR (Fig. 5C). The multiple tumor nodules were shown in Fig. 5D. There were no differences in total body weight, feeding habits, or behavior between the groups, indicating the absence of overt toxicities related to the therapy.

To determine potential mechanisms underlying the efficacy of HA-PLGA (PTX+FAK siRNA)-NPs in tumor tissues, we examined the tumors for antibodies for against FAK (FAK antibody),

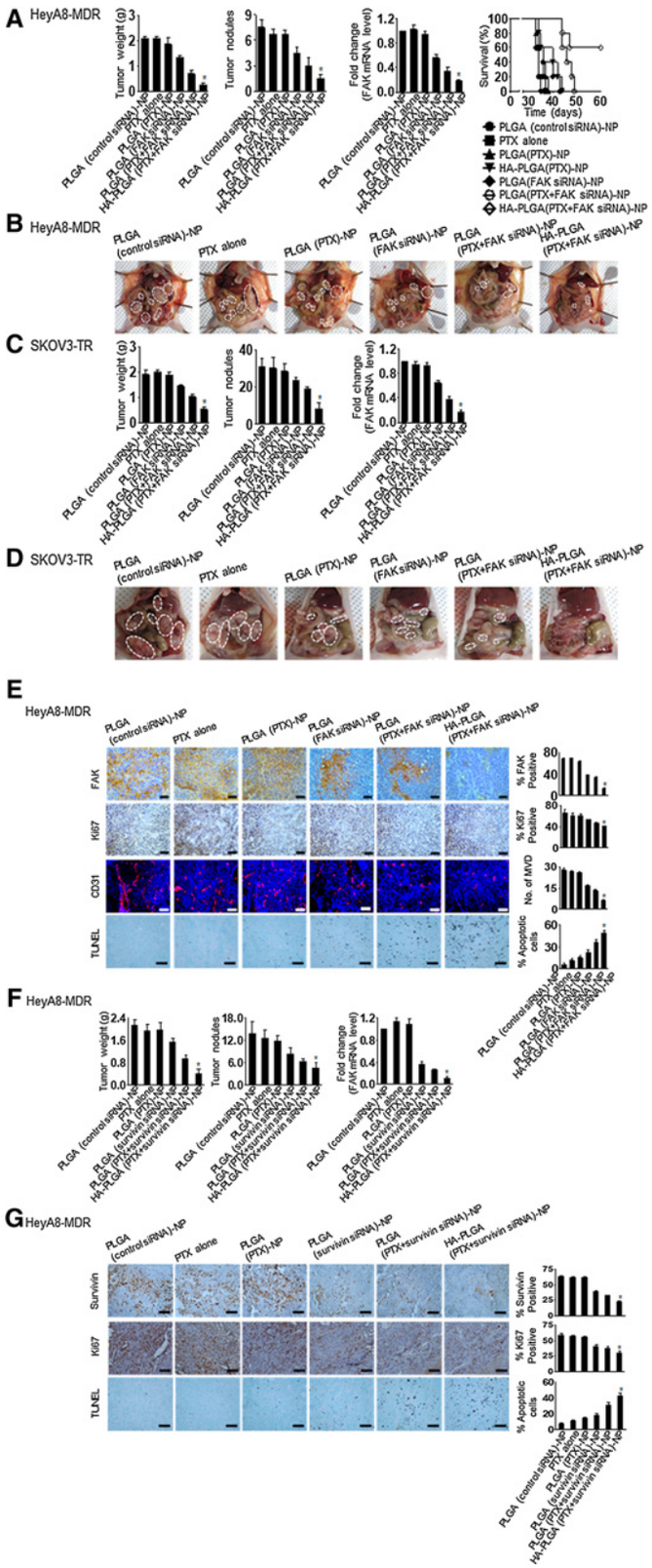

Figure 5.

Therapeutic efficacy of HA-PLGA-NPs in a mouse orthotopic ovarian cancer model. Treatment with HA-PLGA-NPs was started 1 week after intraperitoneal injection of HeyA8-MDR (**A**) and SKOV3-TR (**C**) tumor cells. HA-PLGA (PTX+FAK siRNA)-NPs were injected intravenously twice weekly at doses of 200 μg/kg FAK siRNA and 1.4 mg/kg PTX based on body weight. The fold change in levels of FAK mRNA represents the mean of the triplicates evaluated by qRT-PCR. Photographs of multiple tumor nodules in the HeyA8-MDR (**B**) and SKOV3-TR (**D**) tumor model. **E,** Immunohistochemistry analyses for markers of FAK expression (FAK antibody), cell proliferation (Ki67), microvessel density (MVD and CD31), and TUNEL were performed on HeyA8-MDR tumor tissues following treatment with HA-PLGA-NPs (scale bar, 50 μm). **F,** Treatment with HA-PLGA (PTX + survivin siRNA)-NPs was started 1 week after the intraperitoneal injection of HeyA8-MDR tumor cells in mice. HA-PLGA-NPs were injected intravenously twice weekly at doses of 200 μg/kg survivin siRNA and 1.4 mg/kg PTX. **G,** Immunohistochemistry analyses for markers of survivin expression (survivin antibody), cell proliferation (Ki67), microvessel density (MVD, CD31), and TUNEL were performed on HeyA8-MDR tumor tissues following treatment with HA-PLGA (PTX+survivin siRNA)-NPs (scale bar, 50 μm). Results represent the mean ± SD. Statistical tests were two-sided and *P* values were evaluated using ANOVA analysis. *, $P < 0.05$.

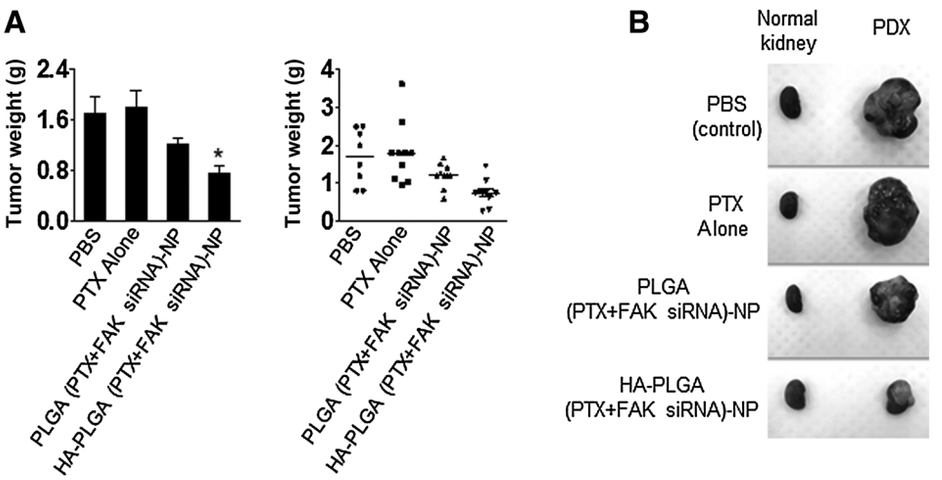

Figure 6.
Therapeutic efficacy of HA-PLGA (PTX+FAK siRNA)-NPs in a chemoresistant PDX tumor model after subrenal implantation into mice. PTX alone, PLGA (PTX+FAK siRNA)-NPs, and HA-PLGA (PTX+FAK siRNA)-NPs were injected intravenously twice weekly at doses of 200 μg/kg FAK siRNA and 1.4 mg/kg PTX. PTX alone was diluted in PBS and injected intravenously twice weekly. **A,** Tumor weight (*, $P < 0.01$). Results represent the mean ± SD. **B,** Representative images of a PDX tumor after treatment.

cell proliferation (Ki67), MVD (CD31), and apoptosis (TUNEL; Fig. 5E). In the HeyA8-MDR model, HA-PLGA (PTX+FAK siRNA)-NP treatment significantly silenced FAK expression ($P < 0.001$), inhibited cell proliferation ($P < 0.01$), and MVD ($P < 0.001$), and increased apoptosis ($P < 0.001$) compared with PLGA (PTX+FAK siRNA)-NP treatment.

We further confirmed therapeutic efficacy of FAK inhibitor (1,2,4,5-Benzenetetraamine tetrahydrochloride, Y15)-encapsulated HA-PLGA-NPs (Supplementary Fig. S10C). Tumor growth was significantly inhibited after treatment with HA-PLGA (PTX+FAK siRNA)-NPs and HA-PLGA (PTX+FAK inhibitor)-NPs compared with PLGA (control siRNA)-NPs ($P < 0.001$). Notably, siRNA-incorporated HA-PLGA-NPs showed higher therapeutic efficacy than FAK inhibitor incorporated HA-PLGA-NPs (42% reduction, $P < 0.05$).

To establish that the effects of HA-PLGA-NPs are not restricted to one target, we performed *in vivo* experiments with siRNA against additional targets. We targeted survivin because of its prominent role in cancer drug resistance (30). The expression of survivin in tumors is strongly associated with the inhibition of apoptosis and resistance to chemotherapy (31). Mice were randomly allocated to one of following groups ($n = 10$ mice/group): (i) control [PLGA (control siRNA)-NPs)], (ii) PTX alone, (iii) PLGA (PTX)-NPs, (iv) PLGA (survivin siRNA)-NPs, (v) PLGA (PTX+survivin siRNA)-NPs, and (vi) HA-PLGA (PTX+survivin siRNA)-NPs. Tumor growth was significantly inhibited following treatment with HA-PLGA (PTX+survivin siRNA)-NPs compared with treatment with PLGA (PTX+survivin siRNA)-NPs (58% reduction, $P < 0.02$) or the control (82% reduction, $P < 0.001$, Fig. 5F). In addition, the number of nodules were significantly reduced following HA-PLGA (PTX+survivin siRNA)-NPs treatment compared with the control (67% reduction, $P < 0.02$); however, no significant difference was observed between treatment with HA-PLGA (PTX+survivin siRNA)-NPs and PLGA (PTX+survivin siRNA)-NPs ($P < 0.32$, Fig. 5F). After treatment, survivin mRNA levels were found to be significantly lower in the HA-PLGA (PTX+survivin siRNA)-NPs group compared with the other groups. Treatment with HA-PLGA (PTX+survivin siRNA)-NPs significantly silenced survivin expression ($P < 0.001$ vs. control), inhibited cell proliferation ($P < 0.001$ vs. control), and increased cellular apoptosis ($P < 0.001$ vs. control; Fig. 5G).

Therapeutic efficacy of HA-PLGA (PTX+FAK siRNA)-NPs in an ovarian cancer PDX model

PDX models are attractive preclinical animal models used in drug development. We developed a PDX model through the subrenal implantation of human ovarian cancer tissues (21). In this study, we used a PDX model of a FIGO stage IIIC serous papillary adenocarcinoma grade III. The patient was a 58-year-old woman who received primary debulking surgery, followed by adjuvant chemotherapy with PTX-carboplatin for 6 cycles. Recurrence of the cancer was detected at the 5-month post-therapy follow-up. Clinically, relapse within 6 months after the last platinum-based therapy is defined as platinum-resistant recurrence. We treated the epithelial ovarian cancer PDX model for 4 weeks starting 2 months after the subrenal implantation (passage 5). Tumor growth was significantly inhibited following treatment with HA-PLGA (PTX+FAK siRNA)-NPs compared with PTX alone (58%, $P < 0.001$ vs. PTX alone) or nontargeted PLGA-NPs (38% $P < 0.005$ vs. PLGA-NPs, Fig. 6A and B).

Discussion

In this study, we developed a receptor-selective two-in-one drug delivery carrier system (HA-PLGA-NP) that contains both PTX and FAK siRNA in a double emulsion. This carrier system targets drug-resistant epithelial ovarian cancer (EOC) cells and induces the potent silencing of target genes to improve chemotherapeutic efficacy. In addition, HA-PLGA-NP significantly inhibited tumor growth without significant side effects compared with PTX alone in a PDX model. The two-in-one drug delivery system proposed here simultaneously transports hydrophobic chemotherapeutics and hydrophilic siRNAs to appropriate cell compartments. HA-PLGA-NPs overcome the low aqueous solubility of chemotherapeutics and protect siRNAs from instability and rapid degradation caused by free circulation in the blood. Moreover, our delivery system lead to enhanced concentrations of therapeutic payloads at tumor sites, minimizing concerns regarding off-target effects, and increasing the therapeutic index.

This approach has broad applications for the selective targeting and efficient treatment of chemoresistant tumor cells.

Chemotherapy resistance confounds effective treatments for ovarian and other cancers. Among chemotherapeutic agents, PTX is commonly used for the treatment of ovarian cancer; however, it these cancer cells often have inherent or acquired resistance to PTX (16). Although a number of important targets in chemoresistance tumor cells have been identified, most of these are difficult to target with small-molecule inhibitors or monoclonal antibodies. This limitation prompted us to use RNA interference as a means to targeting FAK or survivin. We recently demonstrated that chitosan (CH)-NPs are effective systemic delivery carriers of siRNA into orthotopic tumors (7, 19, 32). Although CH-NPs mediated the effective delivery of siRNA, they failed to encapsulate chemotherapeutics such as PTX. Therefore, we created a novel NP system that allowed for the encapsulation and targeted delivery of both siRNA and PTX to tumor cells.

A nanoparticle (NP) system can carry a large payload of drugs compared with antibody conjugates (3, 6). Furthermore, NP payloads are frequently located within the particles, and their type and number of these payloads may not affect the pharmacokinetics and biodistribution of the NPs themselves. PLGA-NPs provide an attractive polymeric matrix for payload delivery and are desirable for biological applications due to their low toxicity and high biocompatibility (9), which are key parameters for medical and pharmaceutical applications. These properties make the use of PLGA-NPs for systemic *in vivo* siRNA and PTX delivery highly attractive.

Targeted delivery systems have been designed to increase or facilitate their uptake into target tissues and to protect payloads while inhibiting nonspecific delivery (7). Recent work on targeted NPs has shown that the primary role of the targeting ligands is to enhance the selective cellular uptake of these NPs into tumor cells and to minimize their accumulation in normal tissues (7). The addition of targeting ligands that provide specific interactions between the NP and the target cell surface can play a vital role in the ultimate delivery of NPs. These targeting ligands enable NPs to bind to cell surface receptors and penetrate cells via receptor-mediated endocytosis. In our study, we labeled the surface of PLGA-NPs with HA, which can target CD44 receptors that are overexpressed on tumor cell membranes. HA, a linear polysaccharide of alternating d-glucuronic acid and N-acetyl-d-glucosamine units, plays important roles in cell adhesion, growth, and migration (11). HA internalization is mediated via matrix receptors, including the CD44 receptor (33). Thus, HA conjugated to an NP system can serve as a useful ligand to target CD44 receptors.

In summary, we developed an HA-PLGA-NP system encapsulating both FAK siRNA and PTX to overcome chemoresistance. In addition, we attached HA onto the surface of the PLGA-NPs to target CD44 receptors on tumor cells. This approach provides a therapeutic benefit by helping to overcome the chemoresistance frequently observed in cancer therapy. In future studies, PLGA-NPs that include combinations of PTX with bioavailable FAK kinase inhibitors should be studied and compared with the use of FAK siRNA, since finding the best combination to overcome chemoresistance is of prime importance. Although our result provides a novel mechanism for FAK knockdown using a siRNA-encapsulated nanoparticle-based system to overcome chemoresistance in ovarian cancer, some potential limitations and other signaling pathways should be considered. Whether the mechanism presented here is present in other possible pathways is not known and will require additional work. In this study, we focused on the development of a nanoparticle-based platform to effectively deliver chemotherapeutics and siRNA as a two-in-one system to overcome chemoresistance. Consequently, we suggest that there is great, unexplored, potential in nano-platform technology. Moreover, whether this two-in-one technique can be applicable in a drug-resistant tumor model in a clinical setting will need to be tested and studies will be required to evaluate the application of this mechanism to other tumor types. Nevertheless, our study provides a novel understanding of an NP-based approach as a nanotechnology platform to overcome chemoresistance. Our NP system represents an important strategy for the treatment of chemoresistant EOC and other cancers.

Disclosure of Potential Conflicts of Interest

No potential conflicts of interest were disclosed.

Authors' Contributions

Conception and design: Y. Byeon, W.S. Choi, Y.J. Lee, H.D. Han, Y.-M. Park
Development of methodology: T.H. Kang, B.C. Shin, A.K. Sood, H.D. Han, Y.-M. Park
Acquisition of data (provided animals, acquired and managed patients, provided facilities, etc.): Y. Byeon, J.-W. Lee, J.E. Won, G.H. Kim, M.G. Kim, T.I. Wi, J.M. Lee, H.J. Ahn, H.D. Han
Analysis and interpretation of data (e.g., statistical analysis, biostatistics, computational analysis): Y. Byeon, J.-W. Lee, J.E. Won, T.I. Wi, J.M. Lee, T.H. Kang, I.D. Jung, Y.-J. Cho, H.J. Ahn, B.C. Shin, A.K. Sood, H.D. Han, Y.-M. Park
Writing, review, and/or revision of the manuscript: Y. Byeon, J.-W. Lee, W.S. Choi, Y.J. Lee, A.K. Sood, H.D. Han, Y.-M. Park
Administrative, technical, or material support (i.e., reporting or organizing data, constructing databases): Y.-J. Cho, H.D. Han
Study supervision: H.D. Han, Y.-M. Park

Acknowledgments

This work was supported by National Research Foundation of Korea (NRF) grant funded by the Korea government (NRF-2016R1A5A2012284, NRF-2016R1A2B2007327, and NRF-2015R1A2A2A04003620 to Y.-M. Park, H.D. Han, and Y.J. Lee). This work was also supported by Basic Research Laboratory Program through the National Research Foundation of Korea (NRF) funded by the Ministry of Science, ICT and Future Planning (No. 2013R1A4A1069575 to H.D. Han, T.H. Kang, and I.D. Jung) and a grant from the National R&D program for Cancer Control, Ministry for Health, Welfare and Family Affairs, Republic of Korea (1520100 to H.D. Han, H.J. Ahn, and J.-W. Lee). This work was also supported by American Cancer Society Research Professor Award and R35CA209904 to A.K. Sood).

The costs of publication of this article were defrayed in part by the payment of page charges. This article must therefore be hereby marked *advertisement* in accordance with 18 U.S.C. Section 1734 solely to indicate this fact.

Received December 14, 2017; revised May 10, 2018; accepted August 2, 2018; published first August 16, 2018.

References

1. Agarwal R, Kaye SB. Ovarian cancer: strategies for overcoming resistance to chemotherapy. Nat Rev Cancer 2003;3:502–16.
2. Siegel RL, Miller KD, Jemal A. Cancer Statistics, 2017. CA Cancer J Clin 2017;67:7–30.
3. Livney YD, Assaraf YG. Rationally designed nanovehicles to overcome cancer chemoresistance. Adv Drug Deliv Rev 2013;65:1716–30.
4. Xu X, Xie K, Zhang XQ, Pridgen EM, Park GY, Cui DS, et al. Enhancing tumor cell response to chemotherapy through nanoparticle-mediated

codelivery of siRNA and cisplatin prodrug. Proc Natl Acad Sci U S A 2013; 110:18638–43.
5. Cao ZT, Chen ZY, Sun CY, Li HJ, Wang HX, Cheng QQ, et al. Overcoming tumor resistance to cisplatin by cationic lipid-assisted prodrug nanoparticles. Biomaterials 2016;94:9–19.
6. Kirtane AR, Kalscheuer SM, Panyam J. Exploiting nanotechnology to overcome tumor drug resistance: challenges and opportunities. Adv Drug Deliv Rev 2013;65:1731–47.
7. Han HD, Mangala LS, Lee JW, Shahzad MM, Kim HS, Shen D, et al. Targeted gene silencing using RGD-labeled chitosan nanoparticles. Clin Cancer Res 2010;16:3910–22.
8. Ye H, Karim AA, Loh XJ. Current treatment options and drug delivery systems as potential therapeutic agents for ovarian cancer: a review. Mater Sci Eng C Mater Biol App 2014;45:609–19.
9. Acharya S, Sahoo SK. PLGA nanoparticles containing various anticancer agents and tumour delivery by EPR effect. Adv Drug Deliv Rev 2011; 63:170–83.
10. Han HD, Byeon Y, Kang TH, Jung ID, Lee JW, Shin BC, et al. Toll-like receptor 3-induced immune response by poly(d,l-lactide-co-glycolide) nanoparticles for dendritic cell-based cancer immunotherapy. Int J Nanomedicine 2016;11:5729–42.
11. Lee SJ, Ghosh SC, Han HD, Stone RL, Bottsford-Miller J, Shen DY, et al. Metronomic activity of CD44-targeted hyaluronic acid-paclitaxel in ovarian carcinoma. Clin Cancer Res 2012;18:4114–21.
12. Huang WC, Chen SH, Chiang WH, Huang CW, Lo CL, Chern CS, et al. Tumor Microenvironment-Responsive Nanoparticle Delivery of Chemotherapy for Enhanced Selective Cellular Uptake and Transportation within Tumor. Biomacromolecules 2016;17:3883–92.
13. Park JH, Cho YY, Yoon SW, Park B. Suppression of MMP-9 and FAK expression by pomolic acid via blocking of NF-kappaB/ERK/mTOR signaling pathways in growth factor-stimulated human breast cancer cells. Int J Oncol 2016;49:1230–40.
14. Hao HF, Takaoka M, Bao XH, Wang ZG, Tomono Y, Sakurama K, et al. Oral administration of FAK inhibitor TAE226 inhibits the progression of peritoneal dissemination of colorectal cancer. Biochem Biophys Res Commun 2012;423:744–9.
15. Stone RL, Baggerly KA, Armaiz-Pena GN, Kang Y, Sanguino AM, Thanapprapasr D, et al. Focal adhesion kinase: an alternative focus for anti-angiogenesis therapy in ovarian cancer. Cancer Biol Ther 2014;15:919–29.
16. Kang Y, Hu W, Ivan C, Dalton HJ, Miyake T, Pecot CV, et al. Role of focal adhesion kinase in regulating YB-1-mediated paclitaxel resistance in ovarian cancer. J Natl Cancer Inst 2013;105:1485–95.
17. Haemmerle M, Bottsford-Miller J, Pradeep S, Taylor ML, Choi HJ, Hansen JM, et al. FAK regulates platelet extravasation and tumor growth after antiangiogenic therapy withdrawal. J Clin Invest 2016;126:1885–96.
18. McLean GW, Carragher NO, Avizienyte E, Evans J, Brunton VG, Frame MC. The role of focal-adhesion kinase in cancer - a new therapeutic opportunity. Nat Rev Cancer 2005;5:505–15.
19. Lu C, Han HD, Mangala LS, Ali-Fehmi R, Newton CS, Ozbun L, et al. Regulation of tumor angiogenesis by EZH2. Cancer Cell 2010;18: 185–97.
20. Barata P, Sood AK, Hong DS. RNA-targeted therapeutics in cancer clinical trials: current status and future directions. Cancer Treat Rev 2016;50: 35–47.
21. Kim HS, Yoon G, Ryu JY, Cho YJ, Choi JJ, Lee YY, et al. Sphingosine kinase 1 is a reliable prognostic factor and a novel therapeutic target for uterine cervical cancer. Oncotarget 2015;6:26746–56.
22. Han HD, Cho YJ, Cho SK, Byeon Y, Jeon HN, Kim HS, et al. Linalool-Incorporated Nanoparticles as a Novel Anticancer Agent for Epithelial Ovarian Carcinoma. Mol Cancer Ther 2016;15:618–27.
23. Kwon HJ, Byeon Y, Jeon HN, Cho SH, Han HD, Shin BC. Gold cluster-labeled thermosensitive liposmes enhance triggered drug release in the tumor microenvironment by a photothermal effect. J Control Release 2015;216:132–9.
24. Wang H, Zhao Y, Wu Y, Hu YL, Nan K, Nie G, et al. Enhanced anti-tumor efficacy by co-delivery of doxorubicin and paclitaxel with amphiphilic methoxy PEG-PLGA copolymer nanoparticles. Biomaterials 2011;32: 8281–90.
25. Han HD, Byeon Y, Jang JH, Jeon HN, Kim GH, Kim MG, et al. *In vivo* stepwise immunomodulation using chitosan nanoparticles as a platform nanotechnology for cancer immunotherapy. Sci Rep 2016;6:38348.
26. Kim HS, Han HD, Armaiz-Pena GN, Stone RL, Nam EJ, Lee JW, et al. Functional roles of Src and Fgr in ovarian carcinoma. Clin Cancer Res 2011;17:1713–21.
27. Heo EJ, Cho YJ, Cho WC, Hong JE, Jeon HK, Oh DY, et al. Patient-derived xenograft models of epithelial ovarian cancer for preclinical studies. Cancer Res Treat 2017;49:915–26.
28. West KA, Castillo SS, Dennis PA. Activation of the PI3K/Akt pathway and chemotherapeutic resistance. Drug Resist Updat 2002;5:234–48.
29. Villedieu M, Deslandes E, Duval M, Heron JF, Gauduchon P, Poulain L. Acquisition of chemoresistance following discontinuous exposures to cisplatin is associated in ovarian carcinoma cells with progressive alteration of FAK, ERK and p38 activation in response to treatment. Gynecol Oncol 2006;101:507–19.
30. Vivas-Mejia PE, Rodriguez-Aguayo C, Han HD, Shahzad MM, Valiyeva F, Shibayama M, et al. Silencing survivin splice variant 2B leads to antitumor activity in taxane–resistant ovarian cancer. Clin Cancer Res 2011;17: 3716–26.
31. Garg H, Suri P, Gupta JC, Talwar GP, Dubey S. Survivin: a unique target for tumor therapy. Cancer Cell Int 2016;16:49.
32. Stone RL, Nick AM, McNeish IA, Balkwill F, Han HD, Bottsford-Miller J, et al. Paraneoplastic thrombocytosis in ovarian cancer. N Engl J Med 2012;366:610–8.
33. Rios de la Rosa JM, Tirella A, Gennari A, Stratford IJ, Tirelli N. The CD44-mediated uptake of hyaluronic acid-based carriers in macrophages. Adv Healthc Mater 2017;6.